High-Power 810-nm Passively Mode-Locked Laser Diode With Al-Free Active Region

Quentin Gaimard, Guy Aubin, Kamel Merghem, Michel Krakowski, Olivier Parillaud, Sylvain Barbay, Abderrahim Ramdane

IEEE Photonics Journal
An IEEE Photonics Society Publication

Open Access

High-Power 810-nm Passively Mode-Locked Laser Diode With Al-Free Active Region

Volume 11, Number 1, February 2019

Quentin Gaimard
Guy Aubin
Kamel Merghem
Michel Krakowski
Olivier Parillaud
Sylvain Barbay
Abderrahim Ramdane

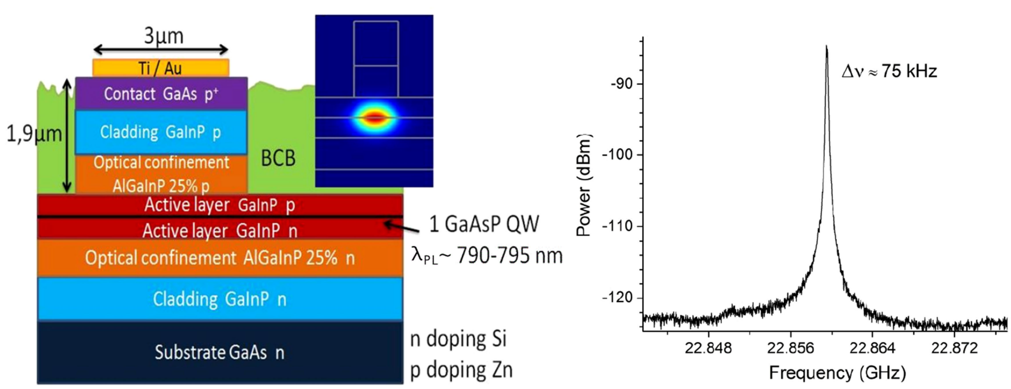

DOI: 10.1109/JPHOT.2018.2886460
1943-0655

High-Power 810-nm Passively Mode-Locked Laser Diode With Al-Free Active Region

Quentin Gaimard,[1] Guy Aubin ,[1] Kamel Merghem,[1] Michel Krakowski,[2] Olivier Parillaud,[2] Sylvain Barbay ,[1] and Abderrahim Ramdane[1]

[1]Centre de Nanosciences et de Nanotechnologies – C2N, CNRS, Univ Paris-Sud, Univ Paris Saclay, Palaiseau 91220, France
[2]III-V Lab, Palaiseau 91767, France

DOI:10.1109/JPHOT.2018.2886460

Manuscript received November 12, 2018; revised December 6, 2018; accepted December 8, 2018. Date of publication December 24, 2018; date of current version February 1, 2019. This work was supported in part by the LabeX LaSIPS (ANR-10-LABX-0032) managed by the French National Research Agency under the "Investissements d'avenir" program (ANR-11-IDEX-0003-02) through the Emergence project LATINO, and in part by the French Renatech Network of clean-room facilities. Corresponding author: S. Barbay (email: sylvain.barbay@c2n.upsaclay.fr).

Abstract: We report on a mode locked semiconductor laser for high-power pulse generation in the 810-nm waveband. This is based on a novel GaAsP/GaInP single quantum-well structure, with Aluminum-free active region. Average output powers higher than 40 mW are reported in narrow ridge two-section devices. A 1.65-mm-long laser with 70 μm saturable absorber yields a stable mode locked regime at a 23-GHz repetition rate as evidenced by a record low RF linewidth of 75 kHz over a wide range of gain currents. Other laser dynamics are also reported at lower frequencies.

Index Terms: Mode-locked laser, near infrared, semiconductor laser diode, Al free.

1. Introduction

The development of low-cost ultrafast pulse laser systems is motivated by the need to replace bulk and expensive sources in a wide range of applications [1], including optical telecommunications [2], [3], signal processing [4], [5], optical tomography [6] and spectroscopy [7]. Their compactness and all-electrical power supply is a major advantage in view of integration in opto-electronic systems. Optical sources with emission around 800 nm are particularly suited for short-haul telecommunications [8], two-photon absorption microscopy [9], and excitation of green fluorescence proteins [10]. Laser pulses with high peak power at this wavelength range could also be an interesting alternative to mode-locked Ti:Sapphire lasers, widely used in many application in photonics for e.g., exploiting non-linear optical effects in non-linear media, for applications to quantum information as optical pumps of GaAs-based micropillar cavities [11], or in novel photonic artificial neural networks applications as ultra-fast sources of input spike trains [12], [13].

The keen interest aroused by such sources at a short wavelength (between 750 nm and 850 nm) is underlined by recent works on semiconductor lasers. 1 GHz repetition rate pulses at 850 nm have been generated using a bi-section semiconductor laser in an external cavity configuration with

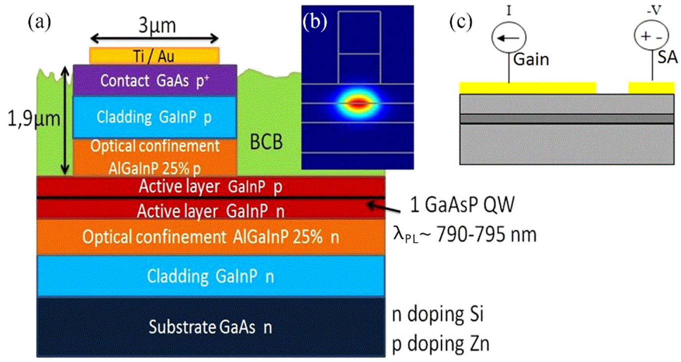

Fig. 1. (a) Epitaxial laser structure and geometry. (b) Numerical calculation of the lateral single-mode confinement. (c) Sketch of the two-section device with forward biased gain section and possibly reverse biased SA section.

intracavity dispersion management in [14]. Integrated designs with AlGaAs quantum wells based bi-section mode-locked lasers have been reported in [15] in a colliding pulse mode locking approach with laser emission at 830 nm and 795 nm and with a repetition rate of 7 GHz, and in [16] with 20 GHz repetition rate and a laser emission wavelength at 760 nm. One particular issue pertains to output power limitations due to inherent catastrophic optical mirror damage in GaAs/ AlGaAs gain media [15]. These authors came up with a specific epitaxial layer design with enlarged vertical mode allowing higher output powers together with improvement in the device reliability. We report here a novel structure with a similar vertical mode size but also based on an Al-free active region that offers an attractive alternative to the conventional AlGaAs quantum-well design, avoiding the creation of oxide on the mirror facets. Devices based on this approach should allow better reliability and longer life time as well as more powerful emission [17].

2. Fabrication

The laser structure is grown on 2” diameter GaAs substrate by Metal Organic Vapor Phase Epitaxy (MOVPE). One GaAsP quantum well of 14 nm thickness is located at the center of a 0.9 μm thick optical cavity made of GaInP. Claddings are made of AlGaInP. A 0.2 μm GaAs highly doped p contact is grown at the top of the structure (figure 1) [17].

We design the laser waveguide for a lateral single-mode confinement as illustrated in figure 1 insert. 2D finite element numerical calculations are used to determine the waveguide width for single-mode operation. The modal effective index neff for a 3 μm wide ridges is 3.34. With such a geometry, the effective vertical mode size d/Γ (with d the well thickness and Γ the optical confinement in the QW) is 0.6 μm.

The shallow ridges are processed by $Cl_2/H_2/O_2$ inductively coupled plasma reactive-ion etching through a Si_3N_4 mask. The devices are planarized and electrically insulated with benzocyclobutene-based polymers (BCB). The p-contact metallization consists of Ti/Au (20 nm/300 nm) formed by electron beam induced deposition. A Ni/Ge/Au/Ni/Au (10 nm/60 nm/120 nm/20 nm/100 nm) ohmic contact is deposited on the n-type layer, followed by a specific Rapid Thermal Annealing (RTA) step, in order to enhance the quality of the contact. Two-section devices, made of a gain and a saturable absorber (SA), are obtained by etching off the p-metallization and p^+-type layers over a 10 μm length. This provides electrical isolation between the two sections. The gain and absorber sections are made of the same active material. The lasers are then mounted with indium on a specific Cu holder. The laser is positioned so that the gain section is place in the front face of the holder. The absorber section is place in the rear face. The gain section and the SA sections are connected with wire bounding to two respective electrodes. No facet coating or passivation is added.

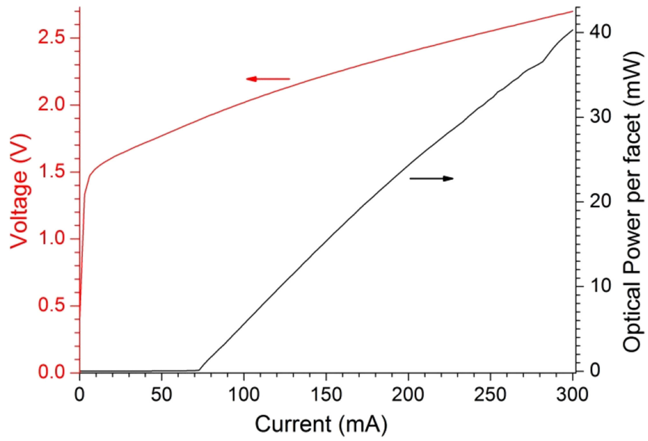

Fig. 2. CW light-current and voltage-current characteristic of a 1.65 mm-long bi-section laser with a 0 V biased 70 μm-long SA recorded at 25 °C.

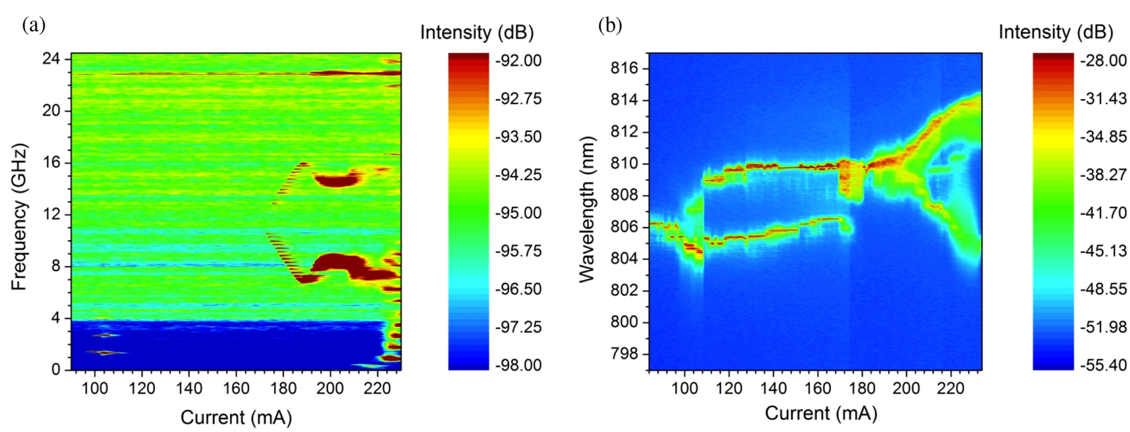

Fig. 3. Mapping in dB scale and versus injected current of (a) the laser output signal RF spectrum measured with a 10MHz RBW, and of (b) the laser optical spectrum with a 0 V absorber bias voltage.

3. Results

The electro-optical characterization of a typical sample is carried out in CW regime at 25 °C with a germanium photodiode in free space. The two-section laser considered hereafter is 1.65 mm-long with a 70 μm-long SA section (4% of the total length). Figure 2 shows the light-current and voltage-current characteristics of the laser without bias on the SA section. The threshold gain current is 72 mA and the average power per facet reaches 40 mW at 300 mA. The threshold current recorded for a single section Fabry-Perot laser of the same dimensions is 45 mA. The measured external efficiency amounts to about 0.18 W/A per facet. On the voltage-current characteristics, we can measure a series resistance of 3 Ω. No thermal roll over is observed up to the maximum tested current of 300 mA.

In two-section lasers the role of the SA section is to allow the generation of optical pulses in the cavity. Their dynamics has been characterized using an external high speed InGaAs photodiode with a 26 GHz −3 dB bandwidth coupled to an Electrical Spectrum Analyzer (ESA). Figure 3(a) shows the RF spectrum of the emitted intensity with injected current from 80 mA to 250 mA. No reverse bias is applied to the SA section. When the injection current is between 114 mA to 176 mA, the RF spectrum exhibits a single sharp peak at 22.8 GHz. This frequency corresponds to the laser repetition rate of the generated pulses. At lower current, three low frequency components are also

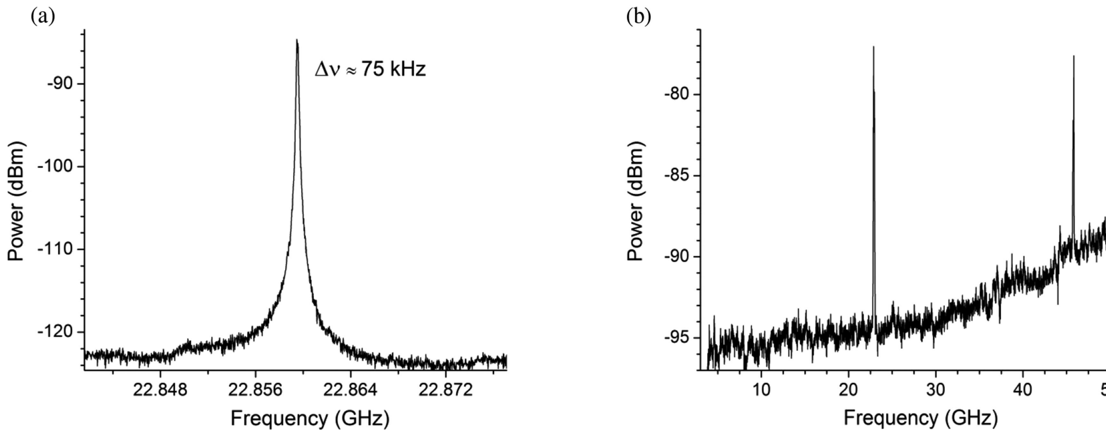

Fig. 4. Laser output signal RF spectrum measured at a gain current of 140 mA and reversed bias of 0 V. (a) RBW = 20 kHz. (b) RBW = 10 MHz.

present. Above 176 mA, two spectral features appear around 8 GHz and 14 GHz and seem to evolve symmetrically with the injected current. Figure 3(b) shows the corresponding optical spectral evolution with the gain current, recorded with a high resolution optical spectrum analyzer. It can be noted that the appearance or extinction of the peak in the RF spectrum corresponds to changes in the optical spectrum. For an injection current from 114 mA to 176 mA, the emitted power is carried by two groups of modes centered around 808 nm, with a 4 nm gap. Out of this range and at lower currents, the emitted power is mainly distributed into the low wavelength group, and at higher ones it is mainly carried in the upper wavelength branch. At much higher current (>200 mA), the spectrum splits again with a gap between the 2 groups of modes, now centered at 810 nm, reaching 10 nm. From the gain bandwidth of one group of modes we calculate a minimum pulse duration of ∼7 ps for Fourier transform pulses. To adjust the absorption recovery time, the SA is then biased to −0.5 V. A reverse bias can in principle modify the laser dynamics and promote the mode locking regime. However, in this case, we record very similar RF and optical spectra.

Considering the main area of interest, from 114 mA to 176 mA, the device exhibits a stable 22.8 GHz RF line over a wide gain range. In this range, the average power varies from 8 mW to 20 mW. The linewidth measured at 140 mA, with an absorber bias at 0 V, is as small as 75 kHz, with more than 35 dB signal-to-noise ratio, with a resolution bandwidth (RBW) of 20 kHz, as shown in Figure 4(a). A 45.6 GHz harmonic component is displayed with an intensity almost similar (1 dB difference at 140 mA) to the fundamental one although affected by the bandwidth-limited photodiode, as shown in Figure 4(b). The upper harmonics could not be observed because of the electrical spectrum analyzer bandwidth. The repetition rate of 22.8 GHz is the time interval between two pulses of 44 ps, which corresponds to the fundamental harmonic of the mode locked regime.

In the other gain areas, the low frequency components, between 1 GHz and 4 GHz, suggest the presence of a Q-switching instability [18], [1], in competition with the mode locking regime.

4. Conclusion

Stable passive mode locking regime has been observed in a novel two-section GaAsP/GaInP quantum well device, with Al-free active region, emitting around 808 nm. The stable mode locking regime is preserved in a large gain current range from 114 mA to 176 mA, corresponding to an average output power from 8 mW to 20 mW, as evidenced by a record low RF linewidth of 75 kHz. In future works, we plan to investigate the impact of HR / AR facet coatings on the laser dynamics and on the output facet emitted power.

References

[1] U. Keller, “Recent developments in compact ultrafast lasers,” *Nature*, vol. 424, pp. 831–838, 2003.
[2] H. Yasaka, Y. Yoshikuni, K. Sato, H. Ishii, and H. Sanjoh, “Multiwavelength lightsource with precise frequency spacing using mode-locked semiconductor laser and arrayed waveguide grating filter,” in *Proc. Opt. Fiber Commun. Conf.*, vol. 19, 1996, pp. 299–300.
[3] S. Kawanishi, “Ultrahigh-speed optical time-division-multiplexed transmission technology based on optical signal processing,” *IEEE J. Quantum Electron.*, vol. 34, no. 11, pp. 2064–2079, Nov. 1998.
[4] P. J. Delfyett *et al.*, “Optical frequency combs from semiconductor lasers and applications in ultrawideband signal processing and communications,” *J. Lightw. Technol.*, vol. 24, no. 7, pp. 2701–2791, 2006.
[5] D. A. B. Miller, “Optical interconnects to silicon,” *IEEE J. Sel. Topics Quantum Electron.*, vol. 6, no. 6, pp. 1312–1317, Nov./Dec. 2000.
[6] J. M. Schmitt, “Optical coherence tomography (OCT): A review,” *IEEE J. Sel. Topics Quantum Electron.*, vol. 5, no. 4, pp. 1205–1215, Jul./Aug. 1999.
[7] A. H. Zewail, “Femtochemistry: Recent progress in studies of dynamics and control of reactions and their transition states.” *J. Phys. Chem.*, vol. 100, no. 31, pp. 12701–12724, 1996.
[8] D. Novak, Z. Ahmed, R. B. Waterhouse, and R. S. Tucker, “Signal generation using pulsed semiconductor lasers for application in millimeterwave wireless links,” *IEEE Trans. Microw. Theory Techn.*, vol. 43, no. 9, pp. 2257–2262, Sep. 1995.
[9] M. Kuramoto, N. Kitajima, H. Guo, Y. Furushima, M. Ikeda, and H. Yokoyama, “Two-photon fluorescence bio imaging with an all semiconductor laser picosecond pulse source,” *Opt. Lett.*, vol. 32, no. 18, pp. 2726–2728, 2007.
[10] P. T. C. So, C. Y. Dong, B. R. Masters, and K. M. Berland, “Two-photon excitation fluorescence microscopy,” *Annu. Rev. Biomed. Eng.*, vol. 2, no. 23, pp. 399–429, 2000.
[11] S. Reitzenstein and A. Forchel, “Quantum dot micropillars,” *J. Phys. D Appl. Phys.*, vol. 43, 2010, p. 033001.
[12] D. Woods and T. J. Naughton, “Photonic neural networks,” *Nature Phys.* vol. 8, pp. 257–259, 2012.
[13] F. Selmi, R. Braive, G. Beaudoin, I. Sagnes, R. Kuszelewicz, and S. Barbay, “Relative refractory period in an excitable semiconductor laser,” *Phys. Rev. Lett.*, vol. 112, no. 18, 2014, Art. no. 183902.
[14] J. C. Balzer, T. Schlauch, A. Klehr, G. Erbert, G. Tränkle, and M. R. Hofmann, “High peak power pulses from dispersion optimised modelocked semiconductor laser,” *Electron. Lett.*, vol. 49, no. 13, pp. 838–839, 2013.
[15] G Tandoi, C. N. Ironside, J. H. Marsh, and A. C. Bryce, “Output power limitations and improvements in passively mode locked GaAs/AlGaAs quantum well lasers,” *IEEE J. Quantum Electron.*, vol. 48, no. 3, pp. 318–327, Mar. 2012.
[16] H. Wang *et al.*, “Ultrashort pulse generation by semiconductor mode-locked lasers at 760 nm,” *Opt. Exp.*, vol. 22, no. 21, pp. 25940–25946, 2014.
[17] M. Krakowski *et al.*, “Review of Al-free active region laser diodes on GaAs for pumping applications,” in *Proc. SPIE*, Quantum Sensing and Nanophotonic Devices XII, 93702C, vol. 9370, 2015.
[18] J. Javaloyes and S. Balle, “Mode-locking in semiconductor Fabry-Pérot lasers,” *IEEE J. Quantum Electron.*, vol. 46, no. 7, pp. 1023–1030, Jul. 2010.